

## Polyoxometalate Embedding of a Tetraruthenium(IV)-oxo-core by Template-Directed Metalation of $[\gamma\text{-SiW}_{10}\text{O}_{36}]^{8-}$ : A Totally Inorganic Oxygen-Evolving Catalyst

Andrea Sartorel,<sup>\*,‡</sup> Mauro Carraro,<sup>‡</sup> Gianfranco Scorrano,<sup>‡</sup> Rita De Zorzi,<sup>†</sup>  
Silvano Geremia,<sup>\*,†</sup> Neal D. McDaniel,<sup>||</sup> Stefan Bernhard,<sup>||</sup> and Marcella Bonchio<sup>\*,‡</sup>

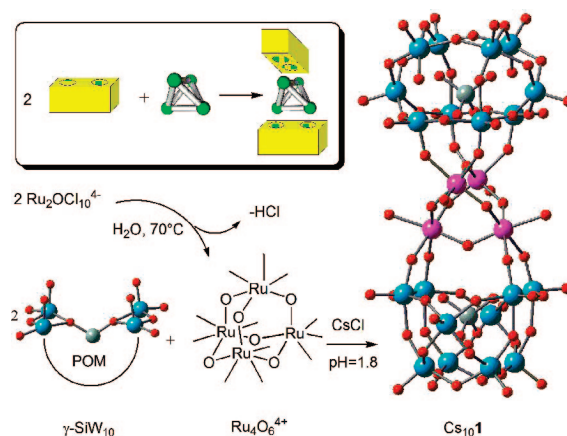
*ITM-CNR and Department of Chemical Sciences, University of Padova, via F. Marzolo 1, 35131 Padova, Italy, Centro di Eccellenza di Biocristallografia, Dipartimento di Scienze Chimiche, Università di Trieste, via L. Giorgieri 1, 34127 Trieste, Italy, and Department of Chemistry, Princeton University, Princeton, New Jersey 08544*

Received October 12, 2007; E-mail: marcella.bonchio@unipd.it; a.sartorel@itm.cnr.it; sgeremia@units.it

The synthesis of tailored multimetal catalysts is becoming increasingly important for high efficiency and multifunctionality in various applications. In particular, polyoxometalates (POMs) provide unique models for the investigation of structure–activity relationships at the borderline between molecules and extended solids.<sup>1,2</sup> In this respect, a research frontier is POM encapsulation of transition metal clusters, whereby redox-active substituents give rise to heterometal-oxo phases, interconnected with the polyoxometalate framework.<sup>1,2</sup> Stabilization of adjacent d-electron centers through multiple- $\mu$ -hydroxo/oxo bridging units is one of the most powerful strategies adopted by natural enzymes to effect multiple/cascade transformations.<sup>3</sup> In the quest for functional, bioinspired catalysts, ruthenium analogues occupy a prominent role, vis-à-vis its unmatched range of accessible oxidation states coupled with some unique mechanistic and selective performance.<sup>4,5</sup> Moreover the electron-withdrawing nature of the POM ligand is predicted to stabilize high-valent intermediates and assist deprotonation equilibria on the polyoxygenated surface.<sup>6,7</sup> Despite their appeal, the synthesis of Ru-substituted POMs poses a major challenge, owing to the inertness of ligand exchange and to purification issues.<sup>8</sup>

We report herein the facile isolation of a new di- $\gamma$ -decaungstosilicate embedding a tetra-ruthenium(IV)-oxo core which shows promise as a water oxidation catalyst.<sup>5</sup>  $\text{Cs}_{10}[\text{Ru}_4(\mu\text{-O})_4(\mu\text{-OH})_2(\text{H}_2\text{O})_4(\gamma\text{-SiW}_{10}\text{O}_{36})_2]$  (**1**) is obtained by reacting the divacant POM,  $[\gamma\text{-SiW}_{10}\text{O}_{36}]^{8-}$  ( $\gamma\text{-SiW}_{10}$ ) with  $\mu$ -oxo-bis-pentachlororuthenate(IV),  $\text{Ru}_2\text{OCl}_{10}^{4-}$ , in aqueous solution (Scheme 1). POM metalation is fostered by the in situ generation of the tetranuclear ruthenium(IV) aqua-ion,  $[\text{Ru}_4\text{O}_6(\text{H}_2\text{O})_n]^{4+}$ , whose existence and adamantane-like solution structure have been proposed on the basis of EXAFS studies.<sup>9</sup> The unprecedented entrapment of the  $\text{Ru}_4\text{O}_6$  fragment occurs readily by the complementary assembly of two  $\gamma\text{-SiW}_{10}$  units under mild temperature conditions. Both the templated vicinal substitution and the lability of the aqua ligands at the ruthenium core,<sup>10</sup> are instrumental for the straightforward formation of **1**. The product precipitates with CsCl in 85% yield; single-crystals suitable for X-ray diffraction are obtained upon recrystallization at pH = 2. The XRD analysis shows a skewed dimeric structure for **1**, where two  $\gamma\text{-SiW}_{10}$  units are connected in a 90° staggered arrangement, by an electrophilic  $[\text{Ru}_4(\mu\text{-O})_4(\mu\text{-OH})_2(\text{H}_2\text{O})_4]^{6+}$  central core. The polyanion has an overall  $D_{2d}$  symmetry

**Scheme 1.** Metalation of  $\text{SiW}_{10}$  by Complementary Lego Assembly of  $[\text{Ru}_4\text{O}_6(\text{H}_2\text{O})_n]^{4+}$



(Scheme 1). The tetraruthenate core displays the expected adamantane-like arrangement, with four ruthenium and six oxygen atoms at the apexes of a tetrahedron and of an octahedron, respectively. The bond valence sum (BVS)<sup>11</sup> calculations, of 4.08(12) for Ru atom, support this description and indicate that two oxygen atoms of the  $\text{Ru}_4\text{O}_6^{4+}$  core are monoprotanated (average bond length of 2.00(2) Å with a BVS of 1.27(4)).

These two symmetry related hydroxo bridges are bent and connect the two adjacent Ru(IV) centers linked to the POM binding site (Ru–O–Ru bond angle of 131.2(9)°). Moreover, they each give rise to a strong three-center H-bond with two proximal Si–O–W bridges (average O–O distance: 2.89(3) Å) (Figure 1). The small BVS values calculated for the terminal oxygen atoms bound to each Ru(IV) center (average coordination length of 2.09(2) Å with BVS of 0.50(4)) are consistent with aqua ligands. Significantly, the  $\gamma\text{-SiW}_{10}\text{Ru}_2$  unit adopts an “out-of-pocket” structural motif, whereby the two adjacent d-electron metals are corner sharing and ligated only by the four oxygen sites of the POM lacuna, with no direct bonding interaction from the internal O–Si tetrahedron.<sup>12</sup> The maintenance of the POM structure in aqueous solution is confirmed by converging evidence, provided by electrospray ionization mass spectra (ESI-MS), resonance Raman (rR), and UV–vis spectroscopy. The ESI-MS spectrum of the water soluble  $\text{Li}_{10}\mathbf{1}$  complex shows envelopes at  $m/z = 1798$  and  $m/z = 1348$  which can be assigned respectively to ions  $[\text{H}_9\text{Ru}_4\text{Si}_2\text{W}_{20}\text{O}_{78}]^{3-}$  and  $[\text{H}_8\text{Ru}_4\text{Si}_2\text{W}_{20}\text{O}_{78}]^{4-}$ , containing the tetraruthenate core after loss

<sup>‡</sup> ITM-CNR and University of Padova.

<sup>†</sup> Dipartimento di Scienze Chimiche, Università di Trieste.

<sup>||</sup> Department of Chemistry, Princeton University.

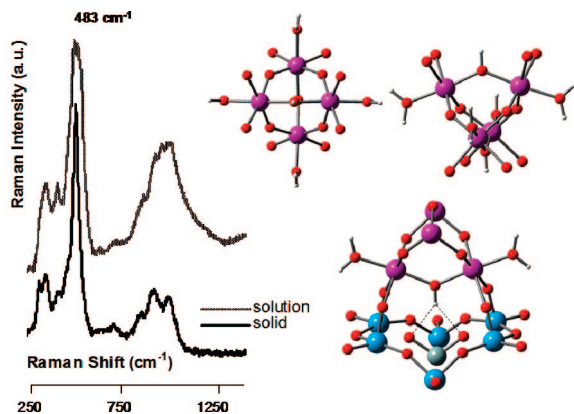


**Figure 1.** The rR spectra of **1**, in the solid state and in H<sub>2</sub>O (pH = 2, excitation at 488 nm). The structures show the top-front views of the central [Ru<sub>4</sub>(μ-O)<sub>4</sub>(μ-OH)<sub>2</sub>(H<sub>2</sub>O)<sub>4</sub>]<sup>6+</sup> fragment.

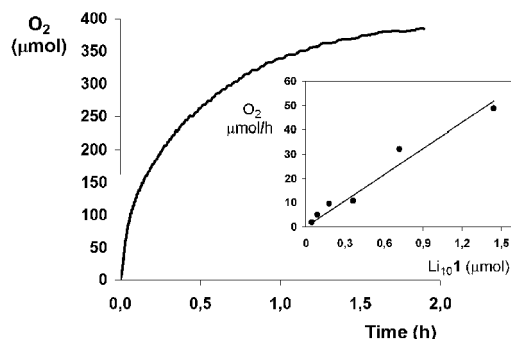


**Figure 2.** Kinetics of O<sub>2</sub> evolution by Li<sub>10</sub>**1**, (4.3 μmol) with Ce(IV) (1720 μmol), in H<sub>2</sub>O (10 mL) at 20 °C. The inset shows a plot of initial rates vs Li<sub>10</sub>**1** (0.045–1.45 μmol), with Ce(IV) (10.9 mmol).

of the four labile water ligands (Supporting Information, Figure S7). Direct evidence for retention of the multiple μ-oxo-ruthenium connectivity is provided by superimposable rR experiments performed for **1**, on a solid sample and in water (pH = 2). Both rR spectra exhibit a prominent feature at 483 cm<sup>-1</sup>, which falls in the range expected for a ν<sub>sym</sub>(Ru–O–Ru) vibrational mode (Figure 1).<sup>5c,13</sup>

The UV–vis spectrum collected in water (pH = 0.6–2.0) shows a sharp absorption band at λ = 443 nm (log ε<sup>443</sup> = 4.57).<sup>9</sup> Acid–base, spectrophotometric titration of Li<sub>10</sub>**1** at λ = 443 nm, and fitting of the ε<sup>443</sup> variation, indicates a reversible mono-protonation equilibrium with a pK<sub>a</sub> of 3.62 (Supporting Information, Figures S4–S6). Structurally related Ru(H<sub>2</sub>O) functions exhibit pK<sub>a</sub> in the range 1.8–3.3.<sup>14</sup> Furthermore, the acid–base equilibrium is not concentration-dependent, thus ruling out POM dissociation or aggregation phenomena. Moreover, the FT-IR spectra are unchanged upon titration of **1**, confirming the maintenance of the POM framework. Multiple-redox states associable to the Ru(IV)<sub>4</sub> core<sup>15,16</sup> and reversible protonation equilibria are critical components for efficient oxygen evolving catalysis, whereby deprotonation of ligated H<sub>2</sub>O triggers the formation of OH<sup>-</sup>/O<sup>2-</sup> reactive sites.<sup>5</sup> Thus, the catalytic activity of Li<sub>10</sub>**1** toward water oxidation has been evaluated by reacting it (4.3 μmol) with an excess of Ce(IV) (1720 μmol), in H<sub>2</sub>O (pH = 0.6) at 20 °C. GC sampling of the reactor headspace, with continuous monitoring of the pressure variation, confirms evolution of molecular oxygen in the system, generating 385 μmol of O<sub>2</sub> in 2 h, with an overall 90% yield on the added oxidant.<sup>16b</sup> A recharge of Ce<sup>IV</sup> induces an equivalent evolution

of oxygen. The water-oxidation rate exhibited by Li<sub>10</sub>**1** is remarkable (maximum TOF > 450 h<sup>-1</sup>, see Figure S9). A linear dependence of the initial rate on [Li<sub>10</sub>**1**] is observed, with a pseudo-first-order kinetic constant of 9.92 × 10<sup>-3</sup> s<sup>-1</sup>, (up to 500 turnovers based on the evolved oxygen, inset in Figure 2 and Figure S10). Its high efficiency is indicative of a very robust catalyst, compared to other previously reported ruthenium systems, bearing classical organic ligands.<sup>5,16b,17</sup> IR, rR spectra confirm the integrity of the POM structure after treatment with Ce(IV) excess (Figures S11–S12). Future studies will investigate the insertion of the Ru<sub>4</sub>O<sub>6</sub> fragment within other POM structures, with the final goal of optimizing the oxygen evolving catalytic performance of the system, in the quest for a modular approach to artificial photosynthesis.<sup>18</sup>

**Acknowledgment.** Financial support from CNR, MIUR (FIRB CAMERE-RBNE03JCR5, PRIN contract no. 2006034372), and the ESF COST D40 action is gratefully acknowledged.

**Supporting Information Available:** Full procedures, spectra, crystallographic data of Cs<sub>10</sub>**1** and kinetics. This material is available free of charge via the Internet at <http://pubs.acs.org>.

## References

- (1) *Polyoxometalate Chemistry from Topology via Self-Assembly to Applications*; Pope, M., Müller, A., Eds.; Kluwer Academic Publishers: Dordrecht, The Netherlands, 2001.
- (2) Long, D.; Burkholder, E.; Cronin, L. *Chem. Soc. Rev.* **2007**, *36*, 105–121.
- (3) (a) Que, L.; Tolman, W. B. *Angew. Chem., Int. Ed.* **2002**, *41*, 1114–1137. (b) DeGrado, W. F.; Di Costanzo, L.; Geremia, S.; Lombardi, A.; Pavone, V.; Randaccio, L. *Angew. Chem., Int. Ed.* **2003**, *42*, 417–420. (c) McEvoy, J. P.; Brudvig, G. W. *Chem. Rev.* **2006**, *106*, 4455–4483.
- (4) (a) Naota, T.; Takaya, H.; Murahashi, S-I. *Chem. Rev.* **1998**, *98*, 2599–2660. (b) Neumann, R.; Dahan, M. *Nature* **1997**, *388*, 353–355.
- (5) (a) Ruttinger, W.; Dismukes, C. *Chem. Rev.* **1997**, *97*, 1–24. (b) Yagi, M.; Kaneko, M. *Chem. Rev.* **2001**, *101*, 21–35. (c) Hurst, J. K. *Coord. Chem. Rev.* **2005**, *249*, 313–328.
- (6) Shaik, S.; Hirao, H.; Kumar, D. *Acc. Chem. Res.* **2007**, *40*, 532–542.
- (7) (a) Sartorel, A.; Carraro, M.; Bagnò, A.; Scorrano, G.; Bonchio, M. *Angew. Chem., Int. Ed.* **2007**, *46*, 3255–3258. (b) Fang, X.; Hill, C. L. *Angew. Chem., Int. Ed.* **2007**, *46*, 3877–3880.
- (8) (a) Bi, L.-H.; Chubarova, E. V.; Nsouli, N. H.; Dickman, M. H.; Kortz, U.; Keita, B.; Nadjjo, L. *Inorg. Chem.* **2006**, *45*, 8575–8583. (b) Artero, V.; Laurencin, D.; Villanneau, R.; Thouvenot, R.; Herson, P.; Gouzerh, P.; Proust, A. *Inorg. Chem.* **2005**, *44*, 2826–2835. (c) Quinonero, D.; Wang, Y.; Morokuma, K.; Khavrutskii, L. A.; Botar, B.; Geletii, Y. V.; Hill, C. L.; Musaev, D. G. *J. Phys. Chem. B* **2006**, *110*, 170–173.
- (9) (a) Osman, J. R.; Crayston, J. A.; Richens, D. T. *Inorg. Chem.* **1998**, *37*, 1665–1668. (b) Heerman, L.; Van Nijen, H.; D’Oliesslager, W. *Inorg. Chem.* **1988**, *27*, 4320–4323.
- (10) The *k<sub>ex</sub>* values of water exchange are 7 order of magnitude higher with respect to the mononuclear aqua ion. Patel, A.; Richens, D. T. *Inorg. Chem.* **1991**, *30*, 3792–3793.
- (11) Brese, N. E.; O’Keeffe, M. *Acta Crystallogr.* **1991**, *B47*, 192–197.
- (12) This coordination mode is an emerging feature documented only for Fe(III) and Cr(III) POMs, see: (a) Botar, B.; Kogerler, P.; Hill, C. L. *Inorg. Chem.* **2007**, *46*, 5398–5403. (b) Botar, B.; Geletii, Y. V.; Kogerler, P.; Musaev, D. G.; Morokuma, K.; Weinstock, I. A.; Hill, C. L. *J. Am. Chem. Soc.* **2006**, *128*, 11268–11277.
- (13) Crystals of Cs<sub>10</sub>**1** are EPR silent, indicating a diamagnetic behavior. Further investigation will address the catalyst evolution to competent species in solution (vide infra).
- (14) Sadakane, M.; Higashijima, M. *Dalton Trans.* **2003**, 659–664.
- (15) The CV of Li<sub>10</sub>**1** in H<sub>2</sub>O (pH = 0.6) shows four anodic and cathodic waves in a potential range from +1.4 to -0.0 V (vs Ag/AgCl) observed at E<sub>1/2</sub> = +1.12, +0.70, +0.53, and +0.29 V with a peak separation of ΔE<sub>p</sub> (= E<sub>pa</sub> - E<sub>pc</sub>) of 89, 98, 59, and 166 mV (Figure S7).
- (16) (a) Electrocatalytic water oxidation by a sandwich-type Ru-POM, (mixture of isomeric clusters) has been reported. Howells, A. R.; Sankarraj, A.; Shannon, C. *J. Am. Chem. Soc.* **2004**, *126*, 12258–12259. (b) K<sub>4</sub>Ru<sub>2</sub>OCl<sub>10</sub>, shows a sluggish reactivity, featuring ca. 20 min induction time, followed by slow oxygen evolution (1 order of magnitude slower than the POM-catalyzed reaction) and soon leveling off to a plateau yield, at <10% of Ce(IV) conversion.
- (17) (a) Sens, C.; Romero, I.; Rodriguez, M.; Llobet, A.; Parella, T.; Benet-Buchholz, J. *J. Am. Chem. Soc.* **2004**, *126*, 7798–7799. (b) Zong, R.; Thummel, R. P. *J. Am. Chem. Soc.* **2005**, *127*, 12802–12803. (c) Liu, F.; Cardolaccia, T.; Hornstein, B. J.; Schoonover, J. R.; Meyer, T. J. *J. Am. Chem. Soc.* **2007**, *129*, 2446–2447.
- (18) Alstrum-Acevedo, J. H.; Brennaman, M. K.; Meyer, T. J. *Inorg. Chem.* **2005**, *44*, 6802–6827.

JA077837F